Systolic blood pressure estimation using PPG and ECG during physical exercise

2016 Physiol. Meas. 37 2154

(http://iopscience.iop.org/0967-3334/37/12/2154)

IOP Publishing | Institute of Physics and Engineering in Medicine Physiological Measurement

Physiol. Meas. **37** (2016) 2154–2169 doi:10.1088/0967-3334/37/12/2154

Systolic blood pressure estimation using PPG and ECG during physical exercise

S Sun[1,2], R Bezemer[1,2], X Long[1,2], J Muehlsteff[2] and R M Aarts[1,2]

[1] Department of Electrical Engineering, Eindhoven University of Technology, Eindhoven, The Netherlands
[2] Philips Research, Eindhoven, The Netherlands

E-mail: shaoxiong.sun@philips.com and sunshxbear@gmail.com

Received 12 April 2016, revised 30 August 2016
Accepted for publication 2 September 2016
Published 14 November 2016

Abstract

In this work, a model to estimate systolic blood pressure (SBP) using photoplethysmography (PPG) and electrocardiography (ECG) is proposed. Data from 19 subjects doing a 40 min exercise was analyzed. Reference SBP was measured at the finger based on the volume-clamp principle. PPG signals were measured at the finger and forehead. After an initialization process for each subject at rest, the model estimated SBP every 30 s for the whole period of exercise. In order to build this model, 18 features were extracted from PPG signals by means of its waveform, first derivative, second derivative, and frequency spectrum. In addition, pulse arrival time (PAT) was derived as a feature from the combination of PPG and ECG. After evaluating four regression models, we chose multiple linear regression (MLR) to combine all derived features to estimate SBP. The contribution of each feature was quantified using its normalized weight in the MLR. To evaluate the performance of the model, we used a leave-one-subject-out cross validation. With the aim of exploring the potential of the model, we investigated the influences of the inclusion of PAT, regression models, measurement sites (finger and forehead), and posture change (lying, sitting, and standing). The results show that the inclusion of PAT reduced the standard deviation (SD) of the difference from 14.07 to 13.52 mmHg. There was no significant difference in the estimation performance between the model using finger- and forehead-derived PPG signals. Separate models are necessary for different postures. The optimized model using finger-derived PPG signals during physical exercise had a performance with a mean difference of 0.43 mmHg, an SD of difference of 13.52 mmHg, and median correlation coefficients of 0.86. Furthermore, we identified two groups of features that contributed more to SBP estimation compared to other features. One group consists of our proposed features

depicting beat morphology. The other comprises existing features depicting the dicrotic notch. The present work demonstrates promising results of the SBP estimation model during physical exercise.

Keywords: photoplethysmography, systolic blood pressure, multiple linear regression, pulse arrival time

(Some figures may appear in colour only in the online journal)

1. Introduction

Blood pressure is one of the vital signs that reflect the cardiovascular status of the human body. Continuous monitoring of blood pressure not only provides immediate physiological parameters for patient care and monitoring, but also reveals health risks that might eventually lead to hypertension or arteriosclerosis (Parati and Valentini 2006). Conventional blood pressure measurements have certain limitations and risks. Measurements using a brachial cuff can be only obtained intermittently. Measurements using a finger cuff is not suitable for long-term use. Measurements using an invasive arterial catheter expose patients to infection risks (Scheer *et al* 2002, Warren *et al* 2006). To avoid these drawbacks and develop alternatives, researchers have been looking for non-invasive continuous blood pressure monitoring methods (Baek *et al* 2010, Monte-Moreno 2011, Ruiz-Rodríguez *et al* 2013).

Photoplethysmography (PPG) has been considered as a method to estimate blood pressure (Baek *et al* 2010, Monte-Moreno 2011, Ruiz-Rodríguez *et al* 2013). It includes an optical sensor that emits light onto the skin and receives the transmitted or reflected light. PPG measures local blood volume changes in tissues at distal sites, such as the finger, forehead, and toe. The relationship between volume and pressure in vessels leads to similar morphology between PPG signals and arterial blood pressure signals. Researchers have therefore proposed a number of features (representing certain physiological properties) to derive blood pressure from PPG signals (Awad *et al* 2007, Millasseau *et al* 2002, Teng and Zhang 2003, Wang *et al* 2009). In addition, other studies were focused on pulse arrival time (PAT) to estimate blood pressure, where PAT is defined as the time delay from the *R* peak in the electrocardiography (ECG) signal to the foot in the PPG signal that immediately follows the *R* peak (Chen *et al* 2000, Poon and Zhang 2005). The underlying mechanism is that, as blood pressure increases, the pulse travels faster in the arteries, leading to a shorter PAT.

In recent years, some researchers have built novel models or improved existing models for estimating blood pressure from PPG. For example, Baek *et al* (2010) investigated a linear model using three features, but that model included a calibration process which required introducing changes in the blood pressure and measuring at least three different blood pressure values. In addition, PPG waveform was not fully explored in that work. Monte-Moreno (2011) proposed and combined a wide range of features from PPG waveforms in order to estimate blood pressure, but that model was only validated in a rest scenario and the proposed features were not explicitly explained. Ruiz-Rodríguez *et al* (2013) designed a model that took raw PPG signal as features and employed a deep learning technique to estimate blood pressure. However, the model was computationally intensive and it was difficult to interpret useful physiological information from PPG waveforms.

In addition to estimation models, different experimental settings were studied. In the work of Baek *et al* (2010), they recorded data during dental anesthesia and during the Valsalva maneuver, where blood pressure was measured either by a catheter or a finger cuff, and PPG was measured at the leg, palm, or finger. In the work of Monte-Moreno (2011), he measured

blood pressure at rest state for each subject by using a sphygmomanometer cuff and measured PPG at the finger. In the work of Ruiz-Rodríguez *et al* (2013), they recorded data in an intensive care unit, where blood pressure was measured invasively by a catheter, and PPG was measured at the finger.

This study aims to design a model using multiple PPG- and ECG-derived features to estimate SBP for healthy people during physical exercise. In addition, this study explores the dependency of model performance on varying factors. These factors include the use of ECG signals, measurement sites (finger and forehead), and different postures (lying, sitting, and standing). We addressed only systolic blood pressure (SBP) because diastolic blood pressure (DBP) changes only marginally during exercise in healthy people (Palatini 1988).

2. Materials and methods

2.1. Data

In this study, 20 subjects were included in our experiments, where the data from one subject was excluded due to low signal quality. Continuous blood pressure, PPG, and ECG signals were acquired from 19 subjects (14 males and 5 females) with an average age of 28.9 ± 8.6 years (ranging from 22 to 53), an average height of 175.6 ± 10.0 cm, and an average weight of 70.6 ± 14.2 kg. For each subject, one ECG and two PPG signals (placed at the fingertip and forehead) were recorded with a sampling frequency of 200 Hz and synchronized subsequently. The blood pressure signal was continuously measured at the finger by using a commercial Portapres device (Finapres Medical Systems, Amsterdam, The Netherlands). This device is based on a volume-clamp method where cuff pressure is changed rapidly to maintain constant arterial volume below the cuff. The oscillation of pressure has been found to resemble the intra-arterial pressure wave. This type of device has been well validated and achieved an accuracy of 6.5 ± 2.6 mmHg compared to intra-arterial blood pressure (Parati *et al* 1989). Signal processing and statistical analysis were carried out using MatLab (MathWorks, Natick, USA).

2.2. Experiments

In this work, we analyzed two datasets collected from 19 subjects participating in two experiments described by Proenca *et al* (2010) and Muehlsteff *et al* (2008), respectively.

The first experiment was done when subjects were doing physical exercise. The experiment started with a 5 min baseline phase at rest. After that, subjects were asked to do three sequential cycling exercise. There was a 5 min recovery period between each of these exercise. Three levels of activity were investigated: low intensity of about 25 W, medium intensity of about 45 W, and high intensity of about 65 W. Figure 1(a) illustrates the experimental protocol and shows an example of SBP changes during physical exercise with the three levels of activity. It can be seen that SBP increased during the exercise periods and decreased during the recovery periods. In addition to this general trend, other variations in the SBP can also be seen. These may be caused by respiration or measurement noise. Although subjects were asked to comply with the protocol as much as possible, the actual exercise periods, therefore the changes in SBP, may still precede or succeed the planned exercise periods. Furthermore, it is possible that subjects cycled too fast and reached the highest SBP early and SBP started to decrease before the exercise stopped and that subjects became excited and had high SBP before the exercise started.

The second experiment was done when subjects changed their postures. During this experiment, all subjects were asked to maintain and change their postures as follows: 5 min

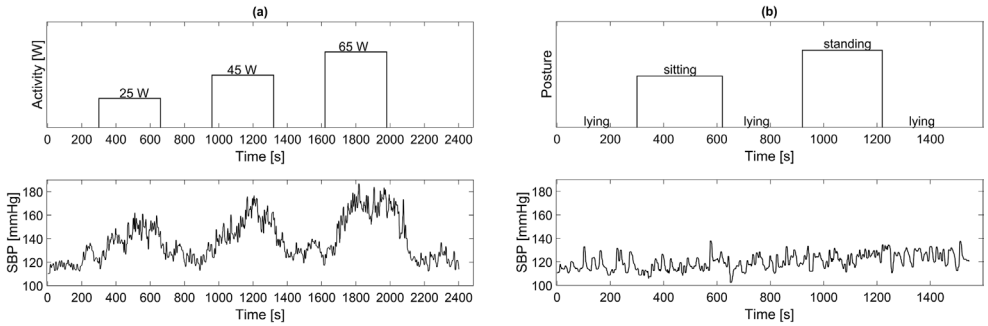

Figure 1. Illustration of study protocols and corresponding systolic blood pressure (SBP) changes. (a) The subjects performed three rounds of cycling activity of different intensities. SBP increased during exercise and decreased during rest. (b) The subjects maintained and changed postures between lying, sitting, and standing.

supine, 5 min sitting, 5 min supine, 5 min standing, and 5 min supine. The analysis of this dataset aimed to investigate the effects of different postures on PPG features and their relation to SBP. Figure 1(b) illustrates the experiment protocol and how SBP responded to different postures.

To mitigate the measurement noise in the first experiment, we instructed the subjects to hold their hands onto a handle bar at a constant height level in respect to the heart level. In the second experiment, we removed the posture transition phases.

2.3. Signal preprocessing

The continuous blood pressure signal was first processed with a six-order Butterworth low-pass filter with a cutoff frequency at 10 Hz. Beat-by-beat SBP values were determined at the detected peaks in the blood pressure signal. For the ECG signal, baseline drift and high frequency noise were removed using a six-order Butterworth band-pass filter with cutoff frequencies at 0.6 Hz and 10 Hz. This was also done on the PPG signal for the same purposes. All filtering processes were implemented in forward and backward directions to eliminate phase distortion. Segments of low quality in the ECG and PPG signals were removed by a combination of visual inspection and dedicated software. This software calculated distances between neighboring detected peaks, distances between neighboring detected valleys, and the amplitude of each detected pulse. By comparing such values with the history values, the program determined the quality of each pulse. The first and second derivatives of the PPG signal were acquired using a smooth noise-robust differentiator (Holoborodko 2008). This method designs a differentiation filter in the frequency domain for the sake of noise robustness. This filter allows for a precise frequency response at low frequencies, and improved suppression of noise at high frequencies. The order of the filter determines suppression effects at high frequency. In this work, we chose the order to be 5. Peaks and valleys in the ECG and PPG signals were detected using the first and second derivative (Baek *et al* 2010, Addison *et al* 2015), which were visually verified afterwards.

2.4. Feature extraction

From a physiological point of view, blood pressure is determined by cardiac output and total peripheral resistance (TPR); arterial stiffness plays a role in increasing TPR. In addition,

Table 1. Features extracted from the PPG waveform, the first and second derivatives, the frequency spectrum, and the arrival time.

Extraction aspects	Features notation (unit)	Description	Number
Waveform see figure 2	PW (s)	Pulse width between half amplitude	1
	SI (—)	Stiffness index: PD divided by subject height	2
	RI (—)	Reflection index: second peak amplitude over first peak amplitude	3
	PAR (—)	Pulse area ratio separated by notch	4
	LVET (s)	Left ventricle ejection time estimated from PPG waveform	5
First derivative see figure 2	dp_{mean} (—)	Mean of normalized first derivative in diastolic phase	6
	dp_{var} (—)	variance of normalized first derivative in diastolic phase	7
	sp_{mean} (—)	Mean of normalized first derivative in systolic phase	8
	sp_{var} (—)	variance of normalized first derivative in systolic phase	9
Second derivative see figure 2	b/a (—)	Height of b over height of a	10
	c/a (—)	Height of c over height of a	11
	d/a (—)	Height of d over height of a	12
	e/a (—)	Height of e over height of a	13
Frequency spectrum	NHA (—)	Normalized harmonic area	14
	SE_{mean} (—)	Mean of spectral entropy	15
	SE_{var} (—)	Variance of spectral entropy	16
	PPGV (—)	PPG pulse amplitude variability	17
	HRV (—)	Heart rate variability	18
Arrival time see figure 2	NPAT (s m^{-1})	Pulse arrival time normalized by subject height	19

blood pressure is regulated by the autonomic nervous system (ANS). Features reflecting the function of ANS are therefore potentially helpful in estimating blood pressure from PPG signals. Similarities between PPG signals and arterial blood pressure signals in their waveform morphologies are often observed. To utilize this similarity, features describing PPG waveform morphology were also included. Therefore we extracted 18 features from the waveform of the PPG signal, the first and second derivatives, and frequency spectrum. In addition, we derived another feature from the arrival time that is related to the time delay from the *R* peak in the ECG signal to the maximum first derivative during upstroke of the pulse in the PPG signal. A summary of all features is given in table 1.

2.4.1. Waveform. Five existing waveform-derived features were computed in this work (see figure 2). Left ventricle ejection time (LVET), the time interval from opening of the aortic valve to its subsequent closure, has been shown to be associated with cardiac output (Finkelstein and Cohn 1993). We estimated LVET, as a feature, from the PPG signal waveform using a multi-Gaussian fitting method, as described by Couceiro *et al* (2012). TPR has been represented as the half amplitude pulse width (PW) (Awad *et al* 2007), the pulse area ratio (PAR)

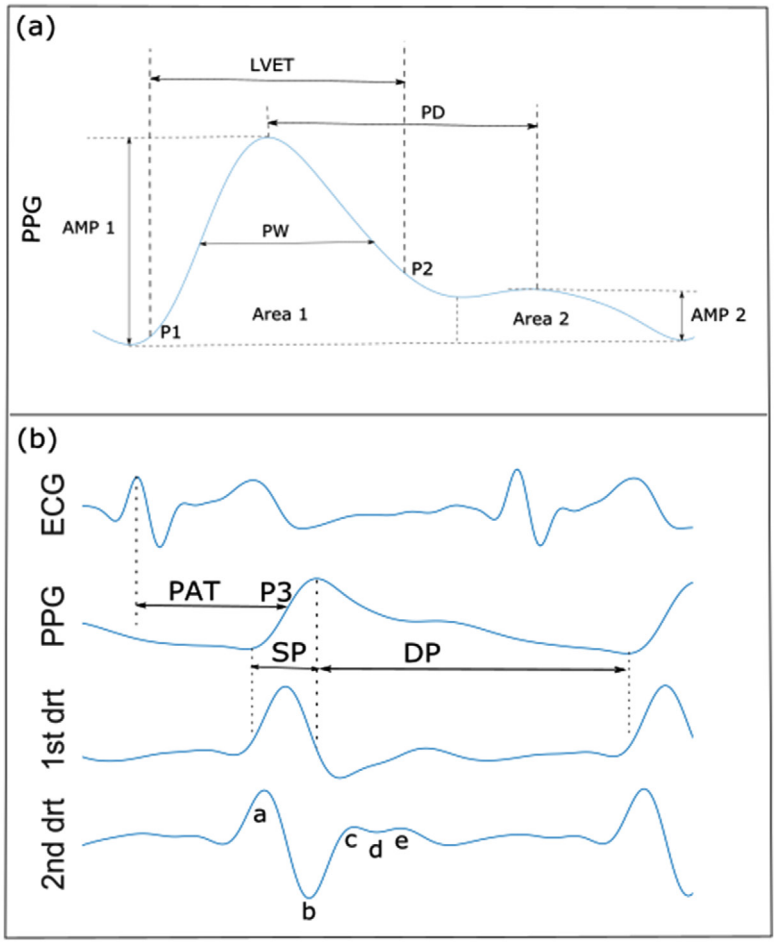

Figure 2. Illustration of the derived features. (a) Features derived from the PPG waveform. P1 and P2 were determined by the method by Couceiro *et al* (2012). (b) The upper panel: features derived from combination of ECG and PPG signals. P3 was the maximum first derivative. The middle panel: features derived from the first derivative of PPG signals. SP stands for systolic phase and DP stands for diastolic phase. The bottom panel: features derived from the second derivative of PPG signals. Waves a and b are the first local maximum and minimum within one pulse, respectively. Waves c and e are the second and third local maximum and d is the local minimum between them. These waves were defined mathematically by Takazawa *et al* (1998).

(Wang *et al* 2010), and the reflection index (RI) (Rubins 2008) of each pulse in the PPG signal. PW was defined as the delay from the half of the amplitude location in the systolic phase to the half of the amplitude location in the diastolic phase. PAR was defined as the ratio between the areas separated by the dicrotic notch, i.e. Area2 divided by Area1. RI was defined as the ratio between the amplitude of the dicrotic peak (AMP2) and that of the first peak (AMP1). When TPR increases, blood flow decreases. In the meantime, the degree of impedance mismatch at reflection sites between large and small arteries is elevated. The decrease in blood flow leads to an enlarged PW and the increased mismatch leads to a stronger reflection effect, which increases RI and PAR. Arterial stiffness also affects blood pressure by altering TPR. As vessels become stiffer, blood pressure increases, the pulse wave travels faster and the delay

between the forward wave and reflected wave drops. Stiffness index (SI) was extracted as the pulse delay (PD) from the first peak to the second peak, normalized by the subject height, as described by Millasseau *et al* (2002).

2.4.2. First derivative. We propose four features from the first derivative of the PPG signal (see figure 2). We derived the first derivative of the PPG signal for each pulse and then a min–max normalization is applied for scaling each pulse waveform to its first peak-to-preceding valley amplitude. This normalization aims to suppress the impact of local perfusion and focus only on the rising and falling characteristics of each pulse. Next, we calculated the mean and variance of the first derivative in the systolic and diastolic phase of the pulse, respectively.

2.4.3. Second derivative. In previous studies (Takazawa *et al* 1998, Hashimoto *et al* 2002, Suzuki and Oguri 2008), five waves were observed in the second derivative and were defined as a–e waves (see figure 2). In these work, features were extracted from the second derivative of the PPG signal such as b/a, c/a, d/a, e/a, and (e-d-c-b)/a that were related to arterial stiffness, or mean blood pressure (MBP). We omitted (e-d-c-b)/a, given that it can be linearly represented by b/a, c/a, d/a, and e/a.

2.4.4. Frequency spectrum. Heart rate variability (HRV) is a proven indicator to reflect ANS. PPG variability (PPGV) has also been shown to be associated with sympathetic vasomotor activities (Nitzan *et al* 1998, Middleton *et al* 2011, Lee *et al* 2013). Thus, HRV and PPGV were included as features in the model where PPGV was derived by calculating PPG amplitude variability. Both features were computed using Welch's technique. The normalized harmonic area (NHA), ratios of the amplitudes at harmonics frequency to the amplitude at the fundamental frequency, was proposed by Wang *et al* (2009) and Yan and Zhang (2005). This feature has been found to be related to pulse wave reflection and SBP by the authors. Thus, we included this feature in the model. In addition, we also included the mean and variance of the spectral entropy in the PPG signal, which were proposed by Monte-Moreno (2011). These features indicate the richness of spectral components and therefore also reflect the damping effects of the pulse during the transmission from the heart to the peripheral. When blood pressure increases, the vessels become stiffer, leading to less damping of the pulse.

2.4.5. Arrival time. PAT consists of a pre-ejection period and a pulse transit time. The pulse transit time from the aorta to the periphery is associated with MBP (Geddes *et al* 1981). As MBP increases, pulse transit time decreases. This relationship is treated as linear for a short period of time when vascular properties are assumed to be stable and therefore the model needs to be adjusted frequently in order to accommodate changes in vascular properties (Chen *et al* 2000). In fact, changes in vascular properties regulated by sympathetic activity, for example vessel radius and vasomotor tone, can be pronounced (Liu *et al* 2014). To take these effects into account and free our model from frequent calibration, we included the above features to reflect the changes in TPR and in sympathetic activity. In this paper, we defined PAT as the delay from the *R* peak in the ECG signal to the maximum in the first derivative of the PPG signal (see figure 2), as a surrogate for the pulse transit time. To mitigate subject-specific pulse travelling distance and make PAT solely dependent on blood pressure, the PAT was normalized by subject height and denoted by NPAT.

2.5. Regression model

In this study, the estimation period was 30 s and all features extracted on a beat-by-beat basis were averaged over that duration. A normalization of all features was done by computing the z-score (standard score). To explore the relationship between the features and the SBP, four regression models were considered, namely multiple linear regression (MLR), linear ridge (LR), random forest (RF), and support vector regression (SVR). MLR has the advantage of displaying a weight for each feature showing its contribution. To quantify and normalize the contribution of each feature, normalized feature weights were calculated by dividing the absolute weight of each feature by the sum of the absolute weights of all involved features. LR penalizes regression coefficients due to highly correlated variables where the penalty parameter was determined using an automatic method proposed in Cule and Iorio (2013). RF utilizes abundant decision trees to reduce variance (the capability of the model when generalized on unseen data) while maintaining low bias (the capability of the model when fitting on the existing data). In this work, we set the total number of trees to be 500 and number of considered features for each node to be 7. SVR maps the feature space to a high-dimensional space, builds linear model on that space, and ignores estimation errors situated within a user-specified distance from the reference values. For SVR, we chose a Gaussian kernel. The results obtained using these four regression models were compared in this work.

2.6. Model validation

To assess the performance of the proposed model, leave-one-subject-out cross validation (LOSOCV) was used. The procedure of employing LOSOCV is shown in figure 3. In each iteration, one set of subject data was withheld to be used as the test data, and the data from the other 18 subjects were used for training the model. The derived model was then applied to the leave-out subject. Performance indicators such as median correlation coefficients, root mean square error (RMSE), and coefficient of determination (R^2) were recorded. R^2 is a statistical measure of how close the data are to the fitted regression model and it shows the percentage of the response variable variation that is explained by the model. When R^2 equals one, it indicates the model explains all the variability of the response data around its mean. When R^2 equals zero, it indicates that the model explains none of the variability of the response data around its mean. When R^2 is less than zero, it indicates that the model is worse than a simple estimation using the mean value. After 19 iterations of these computations, the overall performance was reported by calculating bias (mean of the difference between the measured and estimated SBP), standard deviation (STD) of the difference, median correlation coefficients, R^2, and RMSE. Wilcoxon signed-rank tests were done on median correlation coefficients and RMSE to detect any significant difference.

2.7. Model comparison

We started by considering a model where values of finger PPG-derived features were directly used to estimate SBP, given by

$$\mathrm{SBP}_{i,j} \sim \{f^1_{i,j}, f^2_{i,j}, \ldots, f^{18}_{i,j}\},\ i = 1, 2, \ldots, N_p, j = 1, 2, \ldots, N_m \tag{1}$$

where $\mathrm{SBP}_{i,j}$, $f^1_{i,j}$ are the values of SBP and the feature for the ith subject at the jth measurement, respectively. $\mathrm{SBP}_{i,j}$ is a function of all features $\{f^1_{i,j}, f^2_{i,j}, \ldots, f^{18}_{i,j}\}$.

Then another model applying an initialization at rest was built on the same data, given by

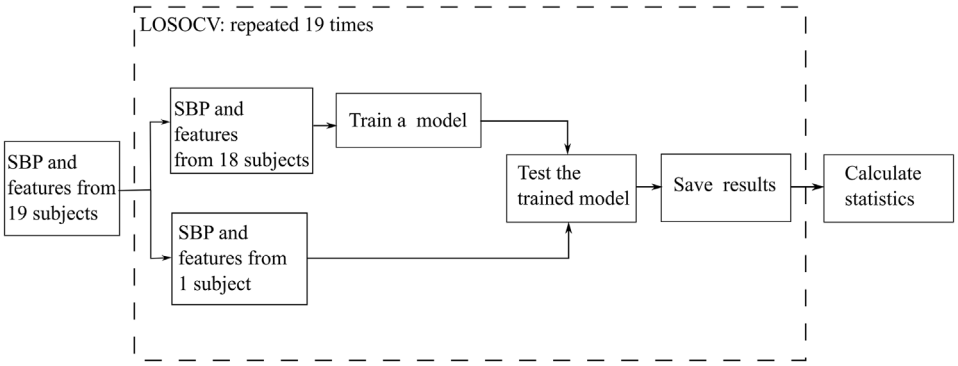

Figure 3. Block diagram of the LOSOCV procedure. In each iteration, one set of subject data was withheld to be used as the test data, and the data of the other 18 subjects were used for training the model. The derived model was then applied to the leave-out subject. Performance indicators were recorded. After all 19 iterations, the performance indicators were computed.

$$\Delta\mathrm{SBP}_{i,j} \sim \left\{\Delta f^1_{i,j}, \Delta f^2_{i,j}, \ldots, \Delta f^{18}_{i,j}\right\} \tag{2}$$

$$\Delta\mathrm{SBP}_{i,j} = \mathrm{SBP}_{i,j} - \mathrm{SBP}_{i,\mathrm{baseline}},\ i = 1,2,\ldots,N_p, j = 1,2,\ldots,N_m \tag{3}$$

$$\Delta f^k_{i,j} = f^k_{i,j} - f^k_{i,\mathrm{baseline}},\ k = 1,2,\ldots,N_f \tag{4}$$

where $\mathrm{SBP}_{i,\mathrm{baseline}}$ and $f^k_{i,\mathrm{baseline}}$ are the SBP value and the kth feature value for the ith subject at the baseline (rest), $\Delta\mathrm{SBP}_{i,j}$ and $\Delta f^k_{i,j}$ are the relative change compared to baseline for SBP and kth feature, respectively.

The initialization was done by collecting SBP and PPG signals during rest periods and averaging them to obtain the baseline values, respectively. During exercise periods, the values of SBP and PPG features were subtracted by their baseline to obtain relative changes. In other words, the model estimated the changes in SBP based on the changes in all features. These two models (with and without initialization) were compared on their estimation performance. Next, the winner of the two models, the initialized model (see results), was provided with an additional feature, NPAT. The model without NPAT and with NPAT was compared with their performance to decide whether to add NPAT in the feature pool. Subsequently, comparisons were made between models using different regression methods: MLR, LR, RF, and SVR. Then the optimal model based on these improvement steps was employed on forehead PPG too and compared with the finger PPG based model. Finally, we investigated the effects of posture change when estimating SBP from PPG signals.

3. Results and discussion

3.1. Physical exercise experiment

The results of estimating SBP using the data from finger PPG without initialization are presented first. All features extracted from finger-derived PPG signals (except for NPAT) were used in the regression model. The median correlation coefficient was 0.83 and the median

Table 2. Model performance for different model settings.

Experiment	Site	Init[a]	NPAT	Performance				
				Bias (mmHg)	STD (mmHg)	Corr.[b] (—)	R^2 (—)	RMSE (mmHg)
Physical exercise	Finger	N	N	0.84	18.61	0.83	0.14	15.27
Physical exercise	Finger	Y	N	0.31	14.07	0.85	0.65	8.99
Physical exercise	Finger	Y	Y	0.43	13.52	0.86	0.62	10.44
Physical exercise	Forehead	Y	Y	0.44	14.00	0.83	0.46	12.30
Posture change	Finger	Y	Y	0.01	7.36	0.47	−0.40	7.33
Posture change	Forehead	Y	Y	−0.89	8.30	0.09	−0.84	6.95

[a] Init.: the initialization process for the model.
[b] Corr.: median correlation coefficients.

RMSE was 15.27 mmHg (see table 2). The estimation performance was improved when initializing the model, leading to a median correlation coefficient of 0.85 and a median RMSE of 8.99 mmHg (see table 2). After performing the significant test, the *p*-values for the median correlation coefficients and RMSE between initialized and uninitialized method were 0.362 and 0.002, respectively (see figure 4). This indicated the better practice of predicting the changes in SBP using changes in the PPG-derived features, rather than directly using their values. This may result from different peripheral conditions such as skin perfusion, and pigmentation that confound the absolute baseline values of PPG readings regardless of SBP (Reisner *et al* 2008).

By incorporating NPAT in the feature pool, the median correlation coefficient was improved to 0.86 (see table 2). The Bland–Altman plot and scatter plot can be found in figure 5 and the normalized weight of each feature can be found in figure 6. After performing the significant test, the *p*-values for the median correlation coefficients and RMSE between the models with and without NPAT were 0.067 and 0.778, respectively (see figure 4). It turned out that the presence of NPAT contributed to the improvement of median correlation coefficients, but it did not help to reduce the RMSE. Several reasons may account for this observation. One might be a lack of consistency of the inter-subject weights for NPAT, which indicates varying vascular properties amongst the subjects. This study intended to compensate this difference by considering features that indicate arterial stiffness such as b/a, and SI in the models, which seemed to be insufficient. Future studies may consider normalizing the pulse arrival time by existing or novel arterial stiffness indexes. In addition, a pre-ejection period (PEP), which is included in the PAT, may confound the relationship between PAT and blood pressure (Payne *et al* 2006). However, one has to include an additional measurement, such as impedance cardiograph to measure PEP, which is beyond the focus of this paper.

Figure 7 compares the estimation results using different regression models. No significant difference was found between MLR and the others in the median correlation coefficients and RMSE. It should be kept in mind that the dataset used in this study was relatively small, which made the models more vulnerable to overfitting. Thus, a larger data set with more subjects should be used in future work to validate these results.

To explore site-dependency of the method, we compared the performance of the model using finger- and forehead-derived PPG signals (see table 2). The results (a median correlation coefficient of 0.83 and a median RMSE of 12.30) were slightly worse than that using finger PPG data, although the differences were found to be not significant ($p > 0.05$), as can be seen in figure 4. This means that the model performed similarly when using finger- or forehead-derived PPG signals. This is a counter-intuitive observation in that PPG signals from cephalic regions (e.g. forehead) are believed to respond more closely to SBP than peripheral regions

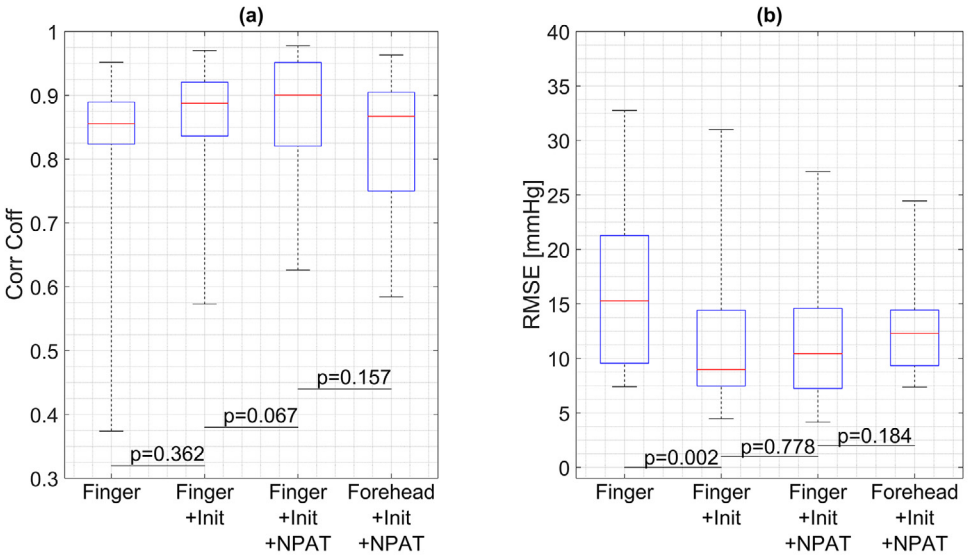

Figure 4. Comparisions of model performance with different settings (a) comparison of correlation coefficients (b) comparsion of RMSE. The p-value from signed-rank test is presented on the solid line. Finger −init −NPAT: without initialization and without NPAT at finger. Finger +init −NPAT: with initialization and without NPAT at finger. Finger +init +NPAT: with initialization and without NPAT at finger. Forehead −init −NPAT: without initialization and with NPAT at foreheads. Horizontal lines: median values. Edges of boxes: the 25th and 75th percentiles. Whiskers: maxia of minia of values.

(e.g. finger), which are richly innervated by the sympathetic nervous system. Several factors may account for this observation. One could be that the reflectance-mode forehead PPG may contain more venous oscillations compared to transmission-mode finger PPG, which confounds arterial blood pressure estimation (Reisner *et al* 2008). Another could be that, during the physical exercise, limbs are better perfused, which makes them more responsive to blood pressure changes. In addition, blood pressure in this paper was measured closer to the finger, which might offer the finger site a slight advantage. Finally, the reflected wave arrives earlier in forehead than in the finger, which sometimes merges with systolic phase causing difficulty in extracting features.

3.2. Posture change experiment

It can be seen in table 2 that the SBP estimation during posture changes was poor (a median correlation coefficient of 0.47 for finger PPG and 0.09 for forehead PPG). Surprisingly, the median RMSE, on the contrary, were better compared to those obtained during physical exercise. But the negative median R^2 values, on the other hand, indicated that they were even worse than the estimation by mean SBP. In fact, the low median RMSE resulted from the much smaller SBP variations in each subject introduced by posture change. The NPAT played a less important role as compared to that in the exercise dataset, especially in forehead PPG. Interestingly, significantly higher correlation coefficients were found when using finger-derived PPG signals than when using forehead-derived PPG signals ($p = 0$). In contrast, RMSE did not show much difference ($p = 0.171$). The poor performance in posture change also reflects the different mechanism of blood pressure change compared to physical exercise.

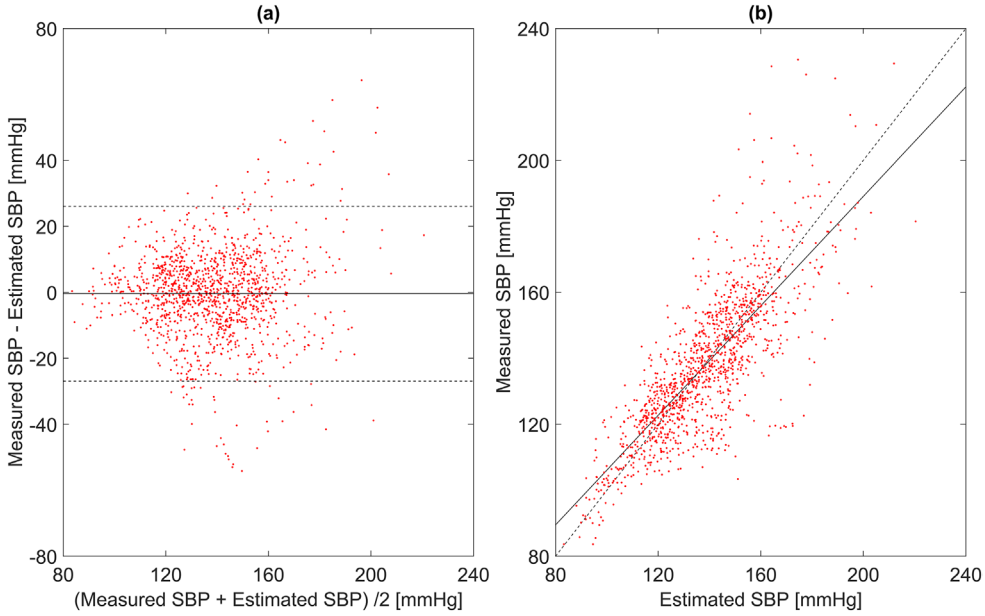

Figure 5. Performance of models built on PPG-derived features in combination with NPAT (a) Bland–Altman plot for estimated and measured SBP using the pooled data from all 19 subjects. The solid line corresponds to bias and the dotted lines correpond to the limits of agreement. (b) Scatter plot for estimated and measured SBP using the pooled data from all 19 subjects. The solid line correponds to the best linear fit and the dotted line is the line of equality.

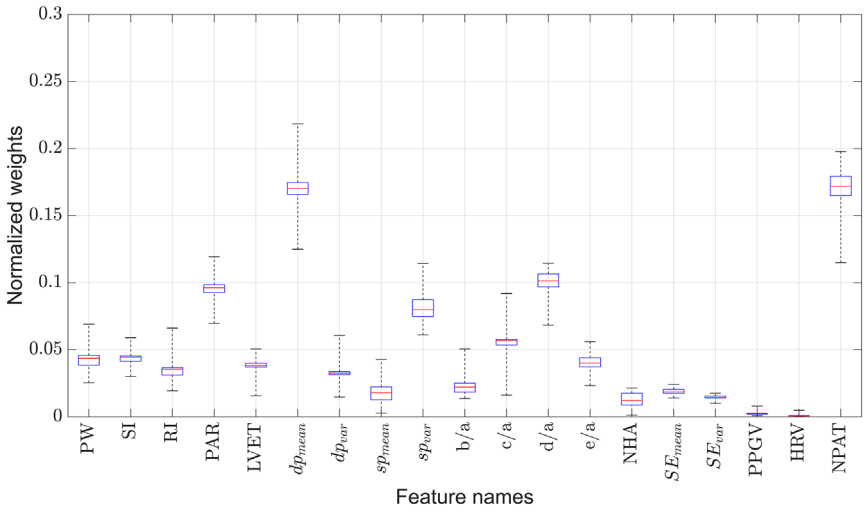

Figure 6. Box plots of the normalized weights for each feature from the trained models after all iterations. The model was built on PPG-derived features in combination with NPAT. Horizontal lines: median values. Edges of boxes: the 25th and 75th percentiles. Whiskers: maxia of minia of values.

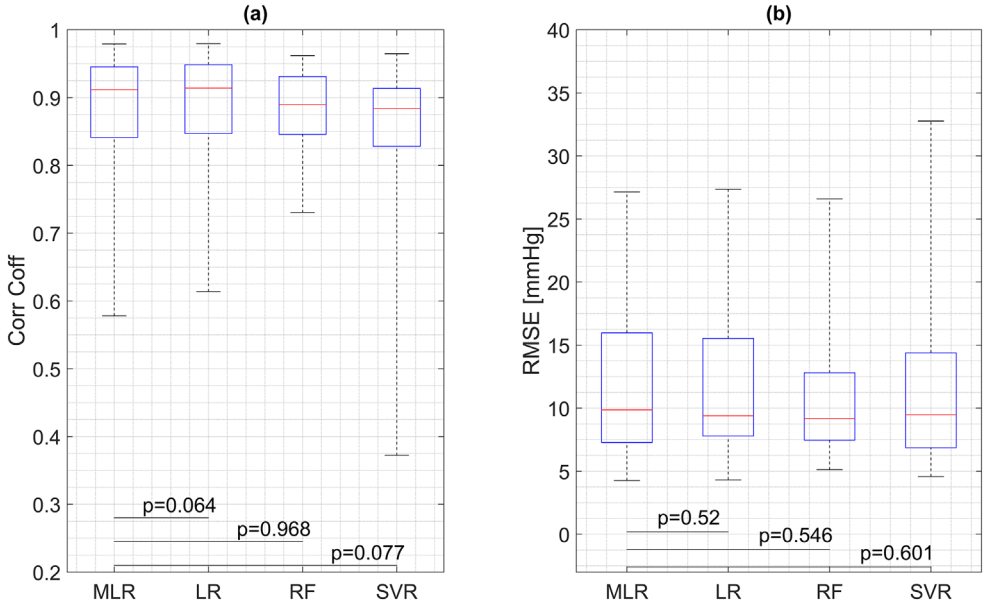

Figure 7. Comparisions between model performances with different regression models (a) comparison of correlation coefficients (b) comparsion of RMSE. The *p*-value from signed-rank test is presented on the solid line. Horizontal lines: median values. Edges of boxes: the 25th and 75th percentiles. Whiskers: maxia of minia of values.

The different weights of features and poor estimation performance suggested that separate models need to be built for different postures during physical exercise.

3.3. Feature contributions

The contributions of the features were evaluated by means of normalized weights for both the physical exercise and the posture change experiments. The normalized weights of five top-ranked features in different settings are shown in table 3. Despite the fact that the feature lists changed with different model settings, dp_{mean}, sp_{var}, RI, PAR, and NPAT seemed to outweigh the other features. The contributions of our proposed features (dp_{mean} and sp_{var}) indicated that these features contained rich information about blood pressure. It should be noted that our proposed features are related to existing features, systolic time and diastolic time, which were defined as the time span in the systolic and diastolic phase of each pulse (Teng and Zhang 2003, Yoon *et al* 2008). When the pulse amplitude is normalized, one can obtain the mean slope of the upstroke (the reciprocal of the systolic time). The same goes for the diastolic time. In contrast, our proposed features (dp_{mean}, dp_{var}, sp_{mean} and sp_{var}) allowed for more descriptions of the morphology of the pulse. Furthermore, both sp_{mean} and dp_{mean} had significantly better correlations with SBP than systolic time and diastolic time, respectively ($p < 0.01$). It is noticeable that dp_{mean}, extracted from diastolic phase, also contributed to SBP estimation. One reason could be that the features extracted from the diastolic phase describe how blood pressure falls, which provides information about the preload. The preload of the preceding pulse determines blood pressure in the next pulse. This finding is in accordance with the work by Teng and Zhang (2003), where diastolic time was found to outperform systolic time when

Table 3. Feature normalized weights for the top five features in the SBP estimation model.

				Features (dimensionless)				
Experiment	Site	Init.[a]	NPAT	1st	2nd	3rd	4th	5th
Physical exercise	Finger	N	N	sp_{var} 0.22	sp_{mean} 0.12	RI 0.11	dp_{mean} 0.10	PAR 0.09
Physical exercise	Finger	Y	N	dp_{mean} 0.21	sp_{var} 0.20	d/a 0.10	PAR 0.08	c/a 0.06
Physical exercise	Finger	Y	Y	NPAT 0.17	dp_{mean} 0.17	d/a 0.10	PAR 0.10	sp_{var} 0.08
Physical exercise	Forehead	Y	Y	RI 0.15	PW 0.13	NPAT 0.13	SI 0.10	NHA 0.09
Posture change	Finger	Y	Y	NPAT 0.19	RI 0.15	sp_{var} 0.14	sp_{mean} 0.11	b/a 0.10
Posture change	Forehead	Y	Y	NHA 0.17	sp_{var} 0.13	RI 0.12	PAR 0.10	b/a 0.09

[a] Init.: the initialization process for the model.

estimating SBP. Interestingly, RI and PAR are related the dicrotic notch, which may indicate that the region close to the notch contains rich information related to SBP.

3.4. Study limitations

There are some limitations in this paper. To begin with, the reference measurement of SBP, by means of finger cuffs, may be less accurate than the measurements from brachial cuffs and invasive arterial lines. However, measurements using brachial cuffs are unable to provide instant and continuous measurements and invasive arterial lines are ethically not acceptable for an experiment with healthy subjects. We therefore took the measurements from finger cuffs as the reference. Second, the signals in this study were acquired in well-controlled experiments: instructing subjects to hold their hands onto a handle bar or removing posture transition phases. By doing so, motion artefacts were substantially suppressed. In reality, motion artefacts can be more disturbing and suppressing them is of importance. Thirdly, even with these controlled experiments, we are not able to control other factors such as contact pressure of the PPG sensor, which may confound PPG signals (Reisner *et al* 2008). Fourthly, the sample size in this paper is relatively small, making the model vulnerable to overfitting. This might explain the finding that advanced regression models discussed in this work did not exhibit advantages over MLR. In addition, we did not select features in this work but we quantified their contributions by means of their normalized weights. Future work may investigate whether feature selection will improve mode performance. Lastly, the best standard deviation we obtained in the physical exercise is 13.52 mmHg, larger than the acceptable threshold of 8 mmHg according to Association for the Advancement of Medical Instrumentation (AAMI 2008). However, one should note that the established protocol by AMMI is mostly applied for individual measurement at rest, rather than tracking blood pressure changes over time. In this small study, we were able to generate a model that only required an initialization at rest, highlighted the contributions of the features and gave promising results.

4. Conclusions

The present study provides an indication of the potential usefulness of an SBP estimation model using PPG and ECG signals for young healthy subjects with a sole requirement of initialization at rest. Particularly, it has been shown that the estimated SBP had high correlations with the measured SBP, while the RMSE still warrants further attention. The initialization reduces the RMSE. The use of PAT can further reduce the STD of difference at the cost of an additional ECG sensor. The model displayed a slightly better tracking capability when using

finger-derived PPG signals as compared to using forehead-derived PPG signals. Subjects should be instructed not to change their postures when applying models in physical exercises and separate models seem necessary for different postures in physical exercise. Overall, the features we propose such as dp_{mean} and sp_{var} played important roles as indicated by the larger normalized weights, and further work can be done on developing features from this normalized derivative domain and employing more advanced models in the context of larger population.

Acknowledgments

This work was financially supported by China Scholarship Council (CSC). The authors wish to express their gratitude to Joaquin Vanschoren for providing advice on machine learning, and to Lars Schmitt and Erik Bresch for reviewing the manuscript.

References

Addison P S, Wang R, Uribe A A and Bergese S D 2015 Increasing signal processing sophistication in the calculation of the respiratory modulation of the photoplethysmogram (DPOP) *J. Clin. Monit. Comput.* **29** 363–72

Association for the Advancement of Medical Instrumentation 2008 Manual, electronic or automated sphygmomanometers *National Standard AAMI SP10-2002/A1:2003/(R) 2008* (Washington, DC: AAMI)

Awad A A, Haddadin A S, Tantawy H, Badr T M, Stout R G, Silverman D G and Shelley K H 2007 The relationship between the photoplethysmographic waveform and systemic vascular resistance *J. Clin. Monit. Comput.* **21** 365–72

Baek H J, Kim K K, Kim J S, Lee B and Park K S 2010 Enhancing the estimation of blood pressure using pulse arrival time and two confounding factors *Physiol. Meas.* **31** 145–57

Chen W, Kobayashi T, Ichikawa S, Takeuchi Y and Togawa T 2000 Continuous estimation of systolic blood pressure using the pulse arrival time and intermittent calibration *Med. Biol. Eng. Comput.* **38** 569–74

Couceiro R, Carvalho P, Paiva R P, Henriques J, Antunes M, Quintal I and Muehlsteff J 2012 Multi-Gaussian fitting for the assessment of left ventricular ejection time from the photoplethysmogram *Proc. 34th Ann. Int. Conf. of the IEEE Engineering in Medicine and Biology Society (San Diego)* pp 3951–4

Cule E and Iorio M D 2013 Ridge regression in prediction problems: automatic choice of the ridge parameter *Genet Epidemiol.* **37** 704–14

Finkelstein S M and Cohn J N 1993 Method and apparatus for measuring cardiac output *US Patent* 5241966

Geddes L A, Voelz M H, Babbs C F, Bourland J D and Tacker W A 1981 Pulse transit time as an indicator of arterial blood pressure *Psychophysiology* **18** 71–4

Hashimoto J, Chonan K, Aoki Y, Nishimura T, Ohkubo T, Hozawa A, Suzuki M, Michimata M, Araki T and Imai Y 2002 Pulse wave velocity and the second derivative of the finger photoplethysmogram in treated hypertensive patients : their relationship and associating factors *J. Hypertens.* **20** 2415–22

Holoborodko P 2008 Smooth noise robust differentiators (www.holoborodko.com/pavel/numerical-methods/numerical-derivative/smooth-low-noise-differentiators/)

Lee Q Y, Redmond S J, Chan G S, Middleton P M, Steel E, Malouf P, Critoph C, Flynn G, O'Lone E and Lovell N H 2013 Estimation of cardiac output and systemic vascular resistance using a multivariate regression model with features selected from the finger photoplethysmogram and routine cardiovascular measurements *Biomed. Eng. Online* **12** 19

Liu Q, Yan B P, Yu C M, Zhang Y T and Poon C C Y 2014 Attenuation of systolic blood pressure and pulse transit time hysteresis during exercise and recovery in cardiovascular patients *IEEE Trans. Biomed. Eng.* **61** 346–52

Middleton P M, Chan G S H, Steel E, Malouf P, Critoph C, Flynn G, O'Lone E, Celler B G and Lovell N H 2011 Fingertip photoplethysmographic waveform variability and systemic vascular resistance in intensive care unit patients *Med. Biol. Eng. Comput.* **49** 859–66

Millasseau S C, Kelly R P, Ritter J M and Chowienczyk P J 2002 Determination of age-related increases in large artery stiffness by digital pulse contour analysis *Clin. Sci.* **103** 371–7

Monte-Moreno E 2011 Non-invasive estimate of blood glucose and blood pressure from a photoplethysmograph by means of machine learning techniques *Artif. Intell. Med.* **53** 127–38

Muehlsteff J, Aubert X A and Morren G 2008 Continuous cuff-less blood pressure monitoring based on the pulse arrival time approach: the impact of posture *Proc. 30th Ann. Int. Conf. of the IEEE Engineering in Medicine and Biology Society (Vancouver)* pp 1691–4

Nitzan M, Babchenko A, Khanokh B and Landau D 1998 The variability of the photoplethysmographic signal–a potential method for the evaluation of the autonomic nervous system *Physiol. Meas.* **19** 93–102

Palatini P 1988 Blood pressure behaviour during physical activity *Sports Med.* **5** 353–74

Parati G, Casadei R, Groppelli A, Di Rienzo M, Mancia G 1989 Comparison of finger and intra-arterial blood pressure monitoring at rest and during laboratory testing *Hypertension* **13** 647–55

Parati G and Valentini M 2006 Prognostic relevance of blood pressure variability *Hypertension* **47** 137–8

Payne R A, Symeonides C N, Webb D J and Maxwell S R J 2006 Pulse transit time measured from the ECG : an unreliable marker of beat-to-beat blood pressure *J. Appl. Physiol.* **100** 136–41

Poon C C Y and Zhang Y T 2005 Cuff-less and noninvasive measurements of arterial blood pressure by pulse transit time *Proc. 27th Ann. Int. Conf. of the IEEE Engineering in Medicine and Biology Society (Shanghai)* pp 5877–80

Proença J, Muehlsteff J, Aubert X and Carvalho P 2010 Is pulse transit time a good indicator of blood pressure changes during short physical exercise in a young population? *Proc. 32th Ann. Int. Conf. of the IEEE Engineering in Medicine and Biology Society (Buenos Aires)* pp 598–601

Reisner A, Shaltis P A, Mccombie D and Asada H H 2008 Utility of the Photoplethysmogram in Circulatory Monitoring *Anesthesiology* **108** 950–8

Rubins U 2008 Finger and ear photoplethysmogram waveform analysis by fitting with Gaussians *Med. Biol. Eng. Comput.* **46** 1271–6

Ruiz-Rodríguez J C *et al* 2013 Innovative continuous non-invasive cuffless blood pressure monitoring based on photoplethysmography technology *Intensive Care Med.* **39** 1618–25

Scheer B, Perel A and Pfeiffer U J 2002 Clinical review: complications and risk factors of peripheral arterial catheters used for haemodynamic monitoring in anaesthesia and intensive care medicine *Crit. Care* **6** 199–204

Suzuki S and Oguri K 2008 Cuffless and non-invasive Systolic Blood Pressure estimation for aged class by using a Photoplethysmograph *Proc. 30th Ann. Int. Conf. of the IEEE Engineering in Medicine and Biology Society (Vancouver)* pp 1327–30

Takazawa K, Tanaka N, Fujita M, Matsuoka O, Saiki T, Aikawa M, Tamura S and Ibukiyama C 1998 Assessment of vasoactive agents and vascular aging by the second derivative of photoplethysmogram waveform *Hypertension* **32** 365–70

Teng X F and Zhang Y T 2003 Continuous and noninvasive estimation of arterial blood pressure using a photoplethysmographic approach *Proc. 30th Ann. Int. Conf. of the IEEE Engineering in Medicine and Biology Society (Vancouver)* pp 3153–6

Wang L, Pickwell-Macpherson E, Liang Y P and Zhang Y T 2009 Noninvasive cardiac output estimation using a novel photoplethysmogram index *Proc. 31th Ann. Int. Conf. of the IEEE Engineering in Medicine and Biology Society (Minneapolis)* pp 1746–9

Wang L, Poon C C Y and Zhang Y T 2010 The non-invasive and continuous estimation of cardiac output using a photoplethysmogram and electrocardiogram during incremental exercise *Physiol. Meas.* **31** 715–26

Warren D K, Quadir W W, Hollenbeak C S, Elward A M, Cox M J and Fraser V J 2006 Attributable cost of catheter-associated bloodstream infections among intensive care patients in a nonteaching hospital *Crit. Care Med.* **34** 2084–9

Yan Y S and Zhang Y T 2005 Noninvasive estimation of blood pressure using photoplethysmographic signals in the period domain *Proc. 27th Ann. Int. Conf. of the IEEE Engineering in Medicine and Biology Society (Shanghai)* vol 4 pp 3583–4

Yoon Y, Cho J H and Yoon G 2008 Non-constrained blood pressure monitoring using ECG and PPG for personal healthcare *J. Med. Syst.* **33** 261–6